MOLECULAR ONCOLOGY 9 (2015) 1720–1735

available at www.sciencedirect.com

ScienceDirect

www.elsevier.com/locate/molonc

Anticancer activity of pyrithione zinc in oral cancer cells identified in small molecule screens and xenograft model: Implications for oral cancer therapy

Gunjan Srivastava[a], *Ajay Matta*[a], *Guodong Fu*[a], *Raj Thani Somasundaram*[a], *Alessandro Datti*[b], *Paul G. Walfish*[a,c,d,e,f], *Ranju Ralhan*[a,c,d,f,*]

[a]*Alex and Simona Shnaider Research Laboratory in Molecular Oncology, Mount Sinai Hospital, Toronto, Canada*
[b]*Simple Modular Assay and Robotics Technology Facility, Lunenfeld Tanenbaum Research Institute, Mount Sinai Hospital, Toronto, Canada*
[c]*Department of Pathology and Laboratory Medicine, Mount Sinai Hospital, Toronto, Canada*
[d]*Joseph and Mildred Sonshine Family Centre for Head and Neck Diseases, Department of Otolaryngology – Head and Neck Surgery, Mount Sinai Hospital, Toronto, Canada*
[e]*Department of Medicine, Endocrine Division, Mount Sinai Hospital and University of Toronto, Toronto, Canada*
[f]*Department of Otolaryngology – Head and Neck Surgery, University of Toronto, Toronto, Canada*

ARTICLE INFO

Article history:
Received 5 May 2015
Accepted 11 May 2015
Available online 21 May 2015

Keywords:
Anticancer agent
High throughput screening
Pyrithione zinc
Oral cancer
Tumor xenografts

ABSTRACT

Oral squamous cell carcinoma (OSCC) patients diagnosed in late stages have limited chemotherapeutic options, underscoring the great need for development of new anticancer agents for more effective disease management. We aimed to identify novel anticancer agents for OSCC using quantitative high throughput assays for screening six chemical libraries consisting of 5170 small molecule inhibitors. In depth characterization resulted in identification of pyrithione zinc (PYZ) as the most effective cytotoxic agent inhibiting cell proliferation and inducing apoptosis in OSCC cells *in vitro*. Further, treatment with PYZ reduced colony forming, migration and invasion potential of oral cancer cells in a dose-dependent manner. PYZ treatment also led to altered expression of several key components of the major signaling pathways including PI3K/AKT/mTOR and WNT/β-catenin in OSCC cells. In addition, treatment with PYZ also reduced expression of 14-3-3ζ, 14-3-3σ, cyclin D1, c-Myc and pyruvate kinase M2 (PKM2), proteins identified in our earlier studies to be involved in development and progression of OSCCs. Importantly, PYZ treatment significantly reduced tumor xenograft volume in immunocompromised NOD/SCID/Crl mice without causing apparent toxicity to normal tissues. Taken together, we demonstrate *in vitro* and *in vivo* efficacy of PYZ in OSCC. In conclusion, we identified PYZ in HTS assays and demonstrated *in vitro* and *in vivo* pre-clinical efficacy of PYZ as a novel anticancer therapeutic candidate in OSCC.

* *Corresponding author*. Joseph and Mildred Sonshine Family Centre for Head and Neck Diseases, Department of Otolaryngology – Head and Neck Surgery Program, Room 413, Joseph & Wolf Lebovic Health Complex, 600 University Avenue, Mount Sinai Hospital, Toronto, Ontario, Canada M5G 1X5. Tel.: +1 416 586 6426; fax: +1 416 586 8861.
E-mail address: rralhan@mtsinai.on.ca (R. Ralhan).
http://dx.doi.org/10.1016/j.molonc.2015.05.005

Abbreviations

PYZ	Pyrithione zinc
APP	Amyloid precursor protein
PKM2	Pyruvate kinase M2
BAX	Bcl-2-associated X protein
BAD	Bcl-2 associated death promoter
PARP	Poly (ADP-ribose) polymerase
PI3K	Phosphatidylinositol-3 kinase
mTOR	Mammalian target of rapamycin
Raptor	Regulatory-associated protein of mTOR
Rictor	Rapamycin-insensitive companion of mTOR
eIF4E	Eukaryotic initiation factor 4E
4EBP1	eIF4E-binding protein 1
SGK1	Glucocorticoid-induced protein kinase 1
PKCα	Protein kinase Cα

1. Introduction

Head and neck squamous cell carcinoma (HNSCC) is among the most lethal cancers and has emerged as one of the leading causes of cancer-related deaths in the world. There are an estimated 263,000 cases of oral squamous cell carcinoma (OSCC) and about 127,000 deaths worldwide each year (Ferlay et al., 2012). Early-stage (I and II) HNSCC patients are treated with surgery and/or radiotherapy, and have five-year survival rates of 70%–90% (Scully and Bagan, 2008). However, two-thirds of HNSCC patients suffer from loco-regional advanced disease (stages III and IV) at the time of diagnosis (Audrey, 2012). Currently, no optimal strategy exists for patients with stage III and IV OSCC. Patients with advanced or recurrent disease have limited treatment options and poor prognosis (Audrey, 2012). Primary surgery and definitive radiotherapy, the only available therapeutic interventions available for OSCC patients, are often associated with considerable detriment to quality of life (Gomez et al., 2009).

Chemo-radiation has emerged as an attractive alternative to traditional surgical management of advanced HNSCC. Chemotherapy (CT) has evolved from palliative care to a central component of curative treatment for locally advanced HNSCC. Cisplatin, carboplatin, methotrexate and taxanes are active as single agents or in combination with radiotherapy in advanced HNSCC (Brana and Siu, 2012). However, dose-limiting toxicities in cancer patients restrict their clinical utility. At present, there is no standard second-line CT regimen for treatment of recurrent and metastatic HNSCC. Monotargeted therapies using inhibitors of epidermal growth factor receptor (EGFR), signal transducer and activator of transcription 3 (STAT3), nuclear factor kappa B (NFκB), and mammalian target of rapamycin (mTOR) have shown limited efficacy (Harari et al., 2009; Martens-de Kemp et al., 2013; Matta and Ralhan, 2009). Thus there exists a great need for development of new drugs for oral cancer. Exploitation of compound collections composed of small novel bioactive molecules is an attractive approach for discovery of new anticancer drugs. In this study, high throughput screening (HTS) of six chemical libraries was used to select compounds possessing anticancer properties against OSCC.

Pyrithione zinc (PYZ), a coordination complex of zinc, is approved by Food and Drug Administration (FDA) as worldwide, over-the-counter, topical antimicrobials for psoriasis and UVB-induced epidermal hyperplasia (Lamore and Wondrak, 2011). PYZ acts as a metal ionophore and increases the intracellular zinc ion concentration. Maintaining the appropriate Zn^{2+} concentration is critical for cell survival since both increased and decreased Zn^{2+} levels can trigger apoptosis in a variety of cell types. Deregulation of zinc homeostasis is also linked to cancer development. Zinc deficiency is associated with poor prognosis of OSCC, esophageal, prostate and breast cancer (Alam and Kelleher, 2012; Carraway and Dobner, 2012; Costello and Franklin, 2011; Kumar et al., 2007; Taccioli et al., 2012). Zn-deficient rats developed tongue, esophageal and fore-stomach tumors when exposed to N-nitrosomethylbenzylamine and 4-nitroquinoline 1-oxide (NQO), while Zn replenishment inhibited tumorigenesis by inducing apoptosis and inhibiting cell proliferation (Fong et al., 2006). Zn supplementation has been reported to improve clinical outcome of patients receiving radiotherapy for HNSCC (Ertekin et al., 2004; Lin et al., 2008, 2009).

In this study we screened libraries consisting of 5170 small molecule inhibitors using HTS assays and identified 48 compounds that selectively killed oral cancer cells. Here, we provide its *in vitro* and *in vivo* evidence that PYZ is an effective cytotoxic agent for OSCC cells.

2. Materials and methods

2.1. Cell culture

Human OSCC cell line, SCC4 was obtained from the American Type Culture Collection (ATCC, Manassas, VA), MDA1986 (Lansford et al., 1999; Myers et al., 2002) was a kind gift from MD Anderson Cancer Centre (Texas, USA) and HSC2 (JCRB0622) was obtained from Health Science Research Resources Bank, Japan (HSRRB). All these cell lines were characterized using short tandem repeat polymorphism analysis and used within 10 passages. Both SCC4 and HSC2 are non-metastatic oral cancer cells of Caucasian and Asian origin, respectively. MDA1986 cells are shown to have metastatic potential (Lansford et al., 1999; Soussi, 2007). SCC4 cells are HPV subtype 6 (–), 16 (–) and 18 (–), and have a point mutation at codon 51 (CCC to *TCC*) (Lui et al., 2013; Masters and Palsson, 1999), HSC2 cells have a mutation in intron 6 of *TP53* (Kim et al., 1993; Sakai and Tsuchida, 1992). MDA1986 cells are HPV 16 (+) and 18 (+), and p53 wild type (Masters and Palsson, 1999). Therefore, these cell lines encompass a range of the characteristics and molecular genotypes found in human head and neck cancers, and were proven to be useful models for our initial study (Ahn et al., 2008; Sawhney et al., 2007). Cells were grown in monolayer cultures in Dulbecco's modified Eagles medium (DMEM) (Invitrogen) supplemented with 10% fetal bovine serum (Sigma–Aldrich, MO) as described earlier (Matta et al., 2010; Tzivion et al., 2006).

2.2. Small molecule inhibitor libraries

A total of 5170 compounds from 6 compound libraries were used for the screening: Prestwick Chemical Library (~1200 compounds), Spectrum (2000 compounds, including many natural products), Kinase Inhibitor library consisting of 320 drugs active against 48 kinases was compiled by Ontario Institute for Cancer Research, Cell Signaling Library (~80 compounds), NIH library (~450 compounds) and Tocris library (~1120 compounds) which includes biologically active molecules, off patent drugs and natural products as described earlier (Grinshtein et al., 2011). Compounds for in depth follow-up studies were obtained from Sigma–Aldrich, MO.

2.3. High throughput screening assays

Primary screening was performed at the Simple Modular Assay and Robotic Technology (SMART) Facility of Lunenfeld Tanenbaum Research Institute (LTRI), Mount Sinai Hospital, Toronto, Canada (Smith et al., 2010). Oral cancer cells (SCC4, HSC2 and MDA1986) were trypsinized and seeded at 1000 cells per well in 50 μl of DMEM medium in 384-well microplates using robotic platform. Compounds were dissolved in dimethylsulfoxide (DMSO) and added using a pin tool to achieve final concentrations of 4 μM–40 μM, using 0.1% DMSO treated cells as controls. After 48 h, Alamar Blue (10 μL) was added and fluorescence intensity was measured after 6 h using PHERAstar microplate reader, equipped with a 540 nm excitation/590 nm emission filter. The dimensionless parameters Z′ and Z-factors were used to assess robustness and consistency of assay (Malo et al., 2006). Normalized data were used to calculate the Z-score and B-score for each compound (Malo et al., 2006). Hits were defined as the active compounds that inhibit the assay signal above a defined threshold value from sample mean signal (Zhang et al., 1999). Confirmatory tests using 10-point, 2-fold serial dilutions of compounds from 40 nM to 20 μM were performed. All experiments were done in triplicate, and data were reported as the mean score ± standard deviation (S.D.). The specific variables of the HTS assay including number of cells, type of media, time course of the assay were optimized before the actual screening (Smith et al., 2010).

2.4. Cell cycle analysis

Cell cycle analysis was performed on a FACScan (BD Biosciences, San Jose, CA) as described earlier (Matta et al., 2010). OSCC cells (SCC4/MDA1986/HSC2) were treated with PYZ (0.5 μM–2.0 μM, 48 h), vehicle (DMSO, 0.1%) or left untreated. After 48 h, cells were washed, harvested, resuspended in PBS, and fixed with 70% ethanol at 4 °C for cell cycle analysis. Cells were washed with PBS (1×, pH = 7.2), treated with ribonuclease A (20 μg/ml) and labeled with propidium iodide (PI).

2.5. Annexin V assay

Apoptosis in PYZ treated and untreated control oral cancer cells (SCC4/HSC2/MDA1986) was evaluated using Annexin V and propidium iodide (PI) double staining as described earlier (Matta et al., 2010).

2.6. Colony formation assay

The anchorage dependent clonogenicity assay was performed using SCC4 cells. Cells (5000 cells/well) were added to 6-well tissue culture plates followed by treatment with PYZ (0.5 μM–2 μM) an additional 6 days. The colonies were fixed and stained with 0.025% crystal violet, washed and counted.

2.7. Cell migration and invasion assay

To determine the effect of PYZ on cell migration and invasion, we performed wound healing and matrigel transwell invasion assays as described (Fu et al., 2013). Briefly, oral cancer cells, SCC4 were plated in 6-well plates following treatment with PYZ (0.5 μM–2 μM) or vehicle (DMSO) for 24 h. A scratch was made on the cell monolayer using a sterile 200 μl pipette tip. After 24 h of treatment, cells were imaged using Olympus microscope and area of the wound was calculated for wound closure in PYZ or vehicle treated cells. Each experiment was done in duplicates.

The cell invasion assay was performed in a 24-well transwell plate (Costar™ Transwell™, Corning INC.). In brief, 20,000 SCC4 cells were plated in upper chamber of transwell plate and treated with varying concentrations of PYZ (0.5 μM–2 μM) or vehicle. The transwells were stained with Hemacolor (EMD Millipore HARLECO™) after 24 h of PYZ treatment and imaged using Olympus microscope. Six random fields were counted and number of cells per field in treated and controls were compared.

2.8. Western blotting

Oral cancer cells (SCC4/MDA1986) were treated with PYZ (0.5 μM–2 μM) or vehicle (DMSO) for 48 h or left untreated. After 48 h, cells were washed in ice-cold phosphate buffered saline (PBS, 1×, pH = 7.2) and lysates were prepared in RIPA lysis buffer containing protease inhibitors (0.02 mg/ml, Roche, Germany). Western blotting was performed according to the procedures as described (Fu and Peng, 2011). The appropriate dilutions of primary antibodies were shown on Supplementary Table T3. Secondary antibodies used were horseradish peroxidase-conjugated goat anti-mouse IgG (dilution 1:2000), anti-rabbit (dilution 1:5000) or anti-goat (dilution 1:5000) obtained from Santa Cruz Biotechnology (Santa Cruz, CA). Detection was performed using the enhanced chemical luminescence method (Pierce, Rockford, IL).

2.9. RNA isolation, cDNA synthesis and realtime quantitative PCR

Total RNA was isolated using the TRizol (Life technology, CA, USA) and reverse transcription was carried out using 1 μg total RNA and Superscriptase III (Life technology, CA, USA) following instructions provided by the manufacturers. The realtime quantitative PCR was performed using gene specific primers and SYBR green on ABI 7900 Realtime PCR System (Applied Biosystems, CA, USA). The primer sequences were sense 5′-TTGGCTGAGGTTGCCGCTGG-3′ and antisense 5′-AGGGCCAGACCCAGTCTGATAG-3′ for 14-3-3ζ; sense 5′-GCCCGAGGAGCTGCTGCAAA-3′ and antisense 5′-

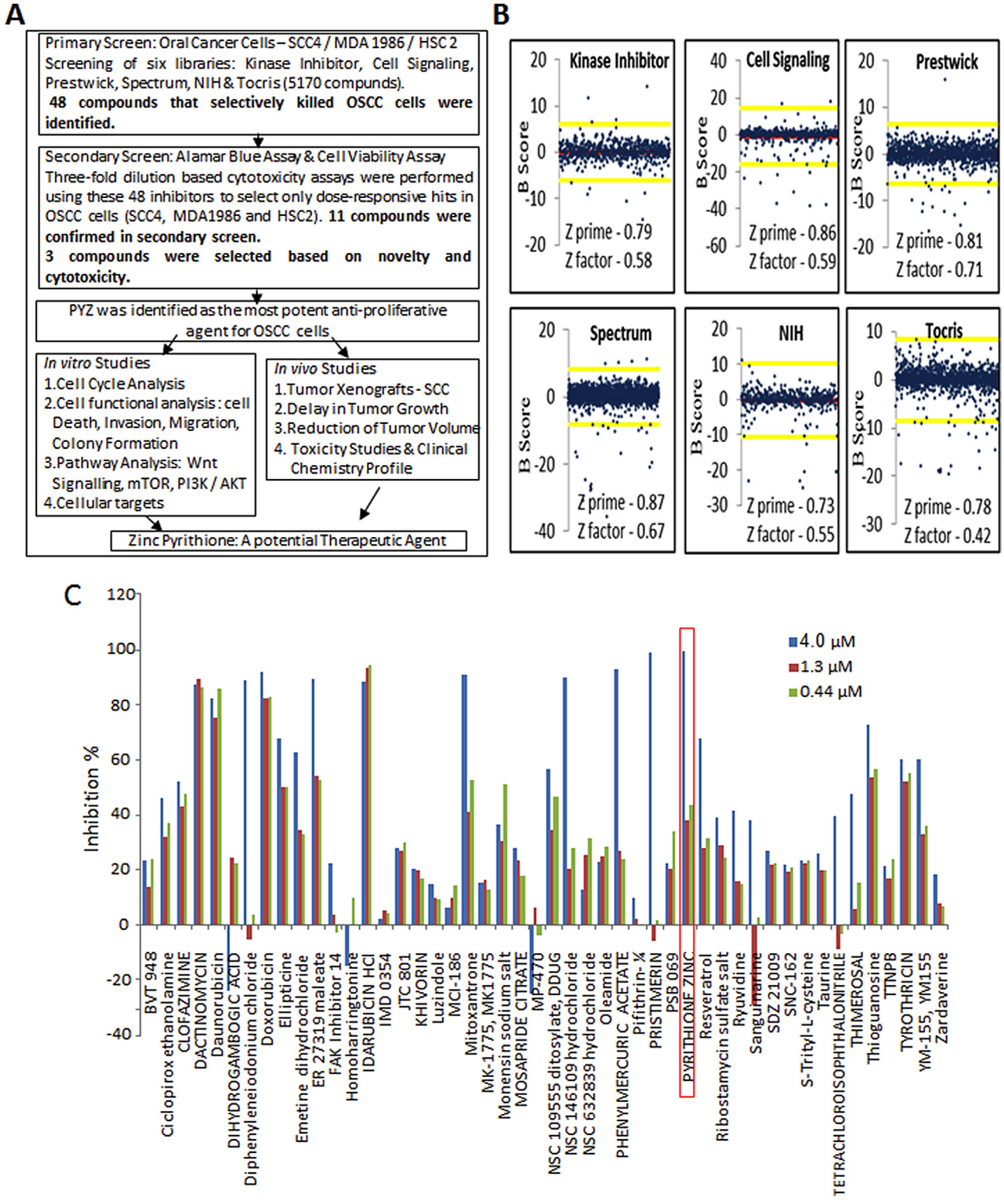

Figure 1 – (A) Work flow of the study. Schematic diagram depicting initial HTS, validation of identified agents in secondary screen and determining the *in vitro* and *in vivo* efficacy of PYZ in OSCC. (B) B-Scores of small molecule inhibitor libraries (Primary screening). B-scores along with Z prime and Z factor of small molecule libraries from Kinase Inhibitor, Cell signaling, Prestwick, Spectrum, NIH and Tocris. Red line indicates the mean score and the yellow lines represent two standard deviations from the mean score. (C) Secondary screening of 48 hits using three concentration gradients in SCC4 cells (High dose – 4 µM, Medium dose – 1.3 µM and Low dose – 0.44 µM). Secondary screening was performed to select only the dose responsive hits.

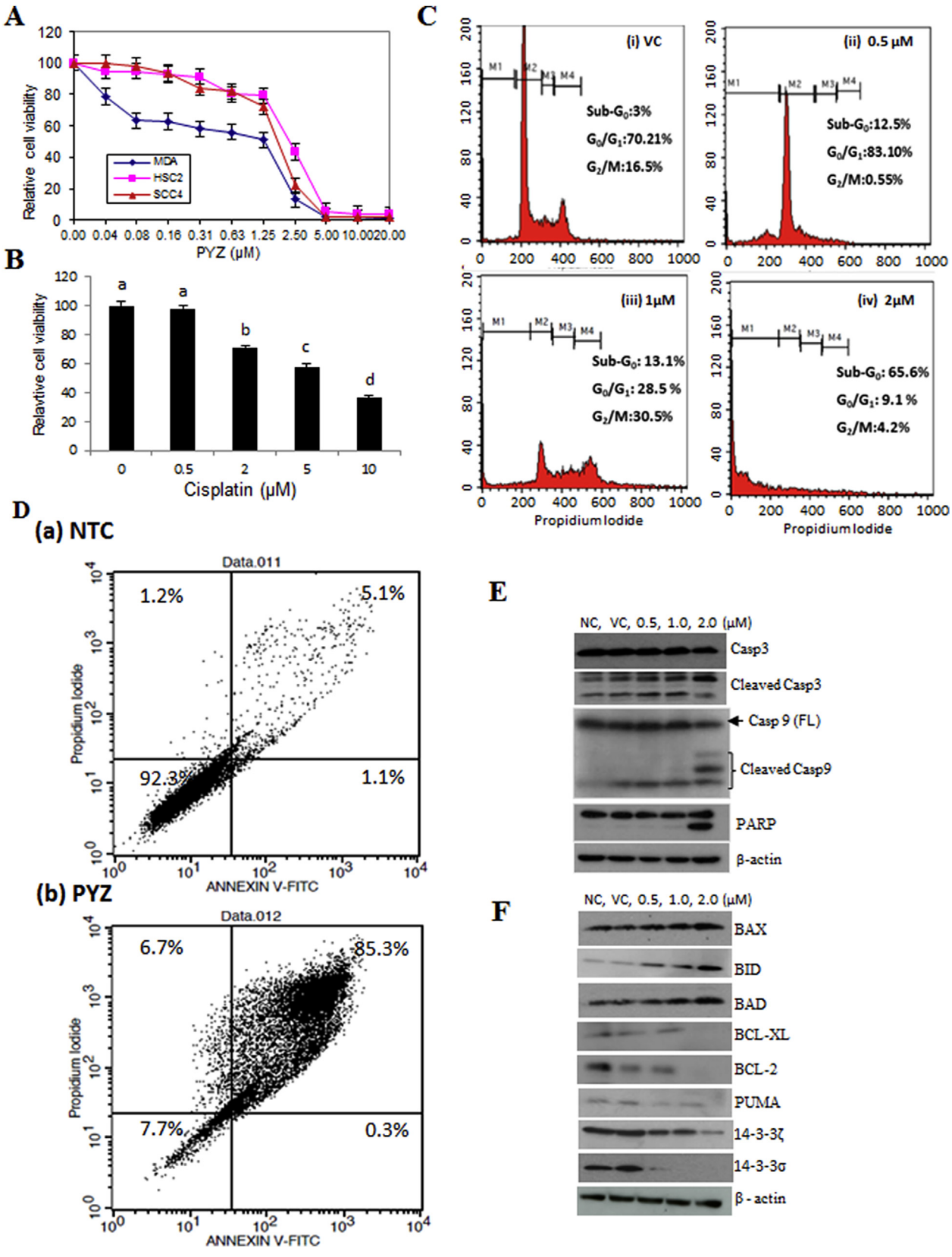

Figure 2 – (A) Dose dependent effect of pyrithione zinc (PYZ). Dose dependent effect of PYZ treatment was determined using 10-point, 2-fold serial dilutions (40 nM–20 μM) on SCC4 (triangle), MDA1986 (diamond) and HSC2 (square). (B) Cisplatin dose dependent effect on SCC4 (0–10 μM). Treatment groups denoted by different letters represent a significant difference at $p < 0.05$ (ANOVA followed by Fisher's LSD test). (C) Cell cycle analysis. Cell cycle analysis was carried out by flow cytometry using propidium iodide (PI) staining for measuring the DNA content of SCC4 cells treated with PYZ for 48 h: (i) vehicle control, (ii) 0.5 μM PYZ, (iii) 1 μM PYZ and (iv) 2 μM PYZ. (D) Annexin V assay. Annexin V

TGCCACCATGGAGGGCGGAT-3′ for cyclin D1; and sense 5′-CAGAGCAAGAGAGGCATCCT-3′ and antisense 5′-TTGAAGGTCTCAAACATGAT-3′ for GAPDH, respectively. Thermocycling conditions include a 10 min reaction at 95 °C followed by 40 cycles of 15 s denaturation at 95 °C and 1 min of annealing and extension at 60 °C. Samples for each treatment group were analyzed in triplicates and experiments were repeated three times. The results of real-time PCR are represented as Ct values, where Ct is a fraction defined as the cycle number at which the sample's fluorescent signal passes a given threshold above baseline. Data analysis was done using ΔCt, the difference in the Ct values derived from the specific genes compared with GAPDH as normalization control.

2.10. Confocal laser scan microscopy (CLSM)

SCC4 cells (1×10^5) were plated on poly-L-lysine-coated coverslips were treated with 2 μM PYZ for 18 h–24 h followed by fixation with 4% paraformaldehyde. Cells were then permeabilized with 0.1% Triton X-100 for 10 min, washed in PBS (1×) and stained with mouse monoclonal β-catenin antibody (dilution 1:200, Abcam, CA). Slides were then incubated with the FITC-labeled secondary antibody and counterstained DAPI (Invitrogen, CA).

2.11. Pyruvate assay

For pyruvate estimation 2×10^6 SCC4 cells treated with different concentrations of PYZ (0 μM, 0.5 μM, 1 μM and 2 μM for 24 h) were harvested and centrifuged at 15,000 g for 5 min at 4 °C. The supernatants were collected for determination of the pyruvate levels using Pyruvate Assay kit (Biovision, CA, USA) according to the manufacturer's instructions.

2.12. Mouse xenograft models

This study was approved by the Animal Ethics Committee of Mount Sinai Hospital prior to commencement and animal care was done in accordance with the Toronto Centre of Phenogenomics (TCP) guidelines. *In vivo* efficacy of PYZ was tested using mouse xenograft models of oral cancer in immunocompromised NOD/SCID/Crl mice which were housed in temperature controlled environment with 12 h light/dark cycles and received food and water *ad libitum*. These mice were injected subcutaneously with 1×10^6 SCC4 cells in right flank using a 27 gauge needle for tumor development. When the average size of tumors reached ~200 mm^3, mice were randomly assigned to 3 groups, 9 mice in each group. Group 1, no treatment control; Group 2, vehicle control (0.05% DMSO); Group 3, treatment group PYZ (1 mg/kg b.wt.). In a pilot experiment using different doses [1, 3 and 5 mg/kg body weight (b.wt.) per week for 6 weeks], we established that PYZ at 1 mg/kg b.wt. did not cause any overt signs of toxicity or any significant weight reduction. This dose was chosen for subsequent experiments. To allow rapid drug absorption and minimize drug-mediated irritation to mice, PYZ was injected intraperitoneal (i.p.) weekly for 6 weeks. Tumor volume and body weight were monitored weekly. At the end of the experiment (or earlier if tumors exceeded 20% body mass), mice were euthanized as per TCP guidelines. Blood was collected from saphenous vein of 3 mice in each group for isolating serum and toxicology studies. Following euthanasia, tumors were harvested and tumor volume was measured 3 times using Vernier callipers. These reading were averaged to obtain mean volume ± S.D. (mm^3). The tissues were subjected to formalin fixed paraffin embedded (FFPE) tissue sections, hematoxylin and eosin staining, and immunohistochemical analysis.

2.13. Immunohistochemistry

Serial FFPE tissue sections (4 μm thickness) of tumors from PYZ treated and vehicle control group mice xenografts were deparaffinized in xylene, hydrated through graded alcohol series, antigen was retrieved by microwave treatment, endogenous peroxidase activity was blocked and non-specific binding was blocked using normal horse serum (10%) as described earlier (Kaur et al., 2014). The sections were incubated with anti-β-catenin antibodies (0.2 μg/ml) (Santa Cruz Biotechnology Inc., Santa Cruz, CA) for 1 h at room temperature. Slides were incubated with biotinylated secondary antibody for 20 min, followed by VECTASTAIN Elite ABC reagent (Vector labs, Burlingame, CA) using diaminobenzidine as the chromogen. Slides were washed with Tris-buffered saline (TBS, 0.1M, pH = 7.4), 3–5 times after every step. Sections were counterstained with Mayer's hematoxylin. In the negative control tissue sections, the primary antibody was replaced by isotype-specific non-immune mouse/rabbit IgG. The sections were evaluated by light microscopic examination. The slides were scanned using Nanozoomer 2.0 (Hamamatsu Photonics K. K., Hamamatsu City, Japan). The image quantitation was carried out using Visiopharm Integrator System software Ver. 4.6.3.857 (Visiopharm, Hoersholm, Denmark).

2.14. Statistical analysis

Data (*in vitro*/*in vivo*) are reported as mean ± S.D. of 3 independent experiments. Values were compared using the Student t-test or with one-way ANOVA when three or more groups were present using GraphPad Prism 6.0 (GraphPad Software). Two-tailed Student t-test was applied for two-group comparison. A $p \leq 0.05$ was considered as statistically significant.

assay carried out after the treatment with 2 μM PYZ in SCC4; PYZ treated cells showed an increase in the fraction of apoptotic cells. (E) Western blot analysis. Panel represents Western blot analysis depicting dose dependent effect of PYZ treatment in SCC4 cells on expression of caspase 3 and increased levels of cleaved caspase 3; caspase 9 and increased levels of cleaved caspase 9; PARP and increased levels of cleaved PARP. β-Actin served as a loading control. (F) Effect of pyrithione zinc on Bcl2 family of apoptosis proteins and 14-3-3 isoform proteins. Treatment with PYZ upregulated the expression of pro-apoptotic proteins – Bax, Bid and Bad, and downregulated the expression of anti-apoptotic proteins – Bcl-xl, PUMA and Bcl2. 14-3-3 isoforms (ζ and σ) were also downregulated in response to PYZ treatment. β-Actin served as a loading control.

3. Results

3.1. Primary screening of novel anticancer agents

In search of novel anticancer agents, we screened six chemical libraries containing 5170 small molecule inhibitors to identify anti-proliferative agents for OSCC cells (SCC4/HSC2/MDA1986). The work flow of this study depicting initial HTS, validation of identified agents in secondary screen and determining the *in vitro* and *in vivo* efficacy of PYZ in OSCC is shown in Figure 1A. The performance characteristics of our cell based-assay for automated HTS were robust with Z'-factor ranging from 0.729 to 0.868. Coefficient of variation (CV) was <7% in our primary screen (Figure 1B). Primary hits were defined as the compounds whose B scores were shifted by at least two standard deviations (99.73% confidence interval) from the mean scores of other compounds. Following these criteria, we identified 48 primary hit compounds that reduced the Alamar Blue signal by 75% as compared to vehicle treated OSCC cells. Our hit rate in this screen experiment is <1%.

3.2. Secondary screening, assay validation and hit identification

In secondary screening, we further prioritized the 48 primary candidates by performing three-fold dilution (4, 1.3 and 0.44 μM) based cytotoxicity assays. To avoid false positives, each dose was used in triplicates and for each cell line the experiments were repeated twice. Compounds were selected based on consistent cytotoxicity in all the three cancer cell lines (SCC4, MDA1986 and HSC2). More than 75% of these primary hits demonstrated good assay quality (Z′ range: 0.808–0.867) confirming their anti-proliferative potency (Figure 1C, Supplementary Figure S1A and S1B). Many of the structurally redundant or known cytotoxic drugs that are being used as anticancer agents were not considered for further analysis. Our secondary screen resulted in verification of 11 of these compounds in OSCC cells. Based on their novelty and dose dependent consistent cytotoxic efficacy in multiple OSCC cell lines, 3 compounds were selected for in depth studies. Of these, PYZ was identified as the most potent anti-proliferative agent for OSCC cell lines causing 94.05%, 99.21% and 99.10% cell death in SCC4, HSC2 and MDA1986 respectively at 4 μM (Figure 1C, Supplementary Figure S1A and S1B). Further, Alamar blue dye reduction assay using 10-point, 2-fold serial dilutions (40 nM–20 μM) revealed a dose dependent decrease in cell viability with an inhibitory concentration at 50% (IC_{50}) of 2 μM at 48 h for SCC4 and HSC2 cells while IC_{50} for MDA was 1.25 μM (Figure 2A). In comparison, cisplatin treatment of SCC4 cells for 48 h also showed dose dependent reduction in cell viability (Figure 2B). Together, we showed the PYZ treatment causes reduced cell viability of OSCC cells.

3.3. Treatment with PYZ induces cell death in OSCC cells

Flow cytometry analysis using propidium iodide (PI) staining was carried out to determine the dose dependent effect of PYZ-treatment (0.5 μM–2 μM, 48 h) on cell cycle of OSCC cells. Significant increase in sub-G_0 fraction of cell cycle was observed in SCC4 (65.6%), HSC2 (52.7%) and MDA1986 (85.7%) cells in comparison with their respective DMSO vehicle control cells (Figure 2C and Supplementary Figure S2A).

Oral cancer cells treated with PYZ (2 μM, 48 h) showed a significant increase in apoptosis from 6.2% to 85.6% in SCC4, from 21.6% to 88.8% in HSC2 and from 16.9% to 93.6% in MDA1986 cells as shown in the flow plot with Annexin V/PI stain (Figure 2D and Supplementary Figure S2B). Furthermore, PYZ treated OSCC cells (SCC4) showed increased levels of cleaved caspase 3, cleaved caspase 9 and cleaved poly ADP-ribose polymerase (PARP) in a dose dependent manner, while the vehicle and no treatment control cells showed a single band of full length caspase 3, caspase 9 and PARP confirming induction of apoptosis in PYZ treated cells (Figure 2E). PYZ treatment also induced cleaved caspase 9 and PARP level in MDA1986 (Supplementary Figure S3). Activation of caspase 9 is regulated by alteration in mitochondrial membrane potential following accumulation of the pro-apoptotic protein, Bad on outer mitochondrial membrane. Western blot analysis showed dose-dependent increase in expression of pro-apoptotic proteins, Bax, Bid and Bad in SCC4 cells treated with PYZ for 48 h (Figure 2F). Furthermore, PYZ-treated SCC4 cells showed decreased levels of Bcl-XL, Bcl-2 and PUMA expression (Figure 2F), as well as two 14-3-3 isoforms (ζ and σ), which are involved in inhibition of apoptosis (Macha et al., 2010) (Figure 2F). Consistently, PYZ treatment also inhibited the expression of 14-3-3 isoforms (ζ and σ) in MDA1986 (Supplementary Figure S3). Densitometry values of protein change by PYZ treatment were also shown by normalization to β-actin control (Supplementary Figure S4A & B). Thus, PYZ treatment results in apoptosis in OSCC cells, with concomitant reduced levels of pro-survival signaling molecules.

3.4. PYZ treatment inhibits colony formation, cell migration and invasion

Treatment with PYZ significantly reduced colony formation of OSCC cells (SCC4) (Figure 3A). To determine the effect of PYZ treatment on migration and invasive potential of OSCC, SCC4 cells were treated with PYZ (0.5 μM and 1 μM) for 24 h as described in Materials and methods. Wound healing assays revealed significant reduction in healing of the wound in PYZ (2 μM) treated SCC4 cells (<5%) in comparison with vehicle control cells in 24 h (Figure 3B). Similarly, there was a significant reduction in invasive capability of SCC4 cells treated with PYZ (0.5 μM–2 μM), for 24 h (Figure 3C). Thus, PYZ leads to reduced colony formation, migration, and invasion of OSCC cells.

3.5. Treatment with PYZ led to altered PKM2 expression

Zinc homeostasis is of vital importance for activity of the glycolytic enzymes, and perturbations in zinc homeostasis will affect the metabolic activity in cancer cells. Hence we measured the pyruvate levels in PYZ treated oral cancer cells as a measure of effect of this drug on glycolysis. Treatment of SCC4 cells with 1.0 μM and 2 μM PYZ for 24 h resulted in

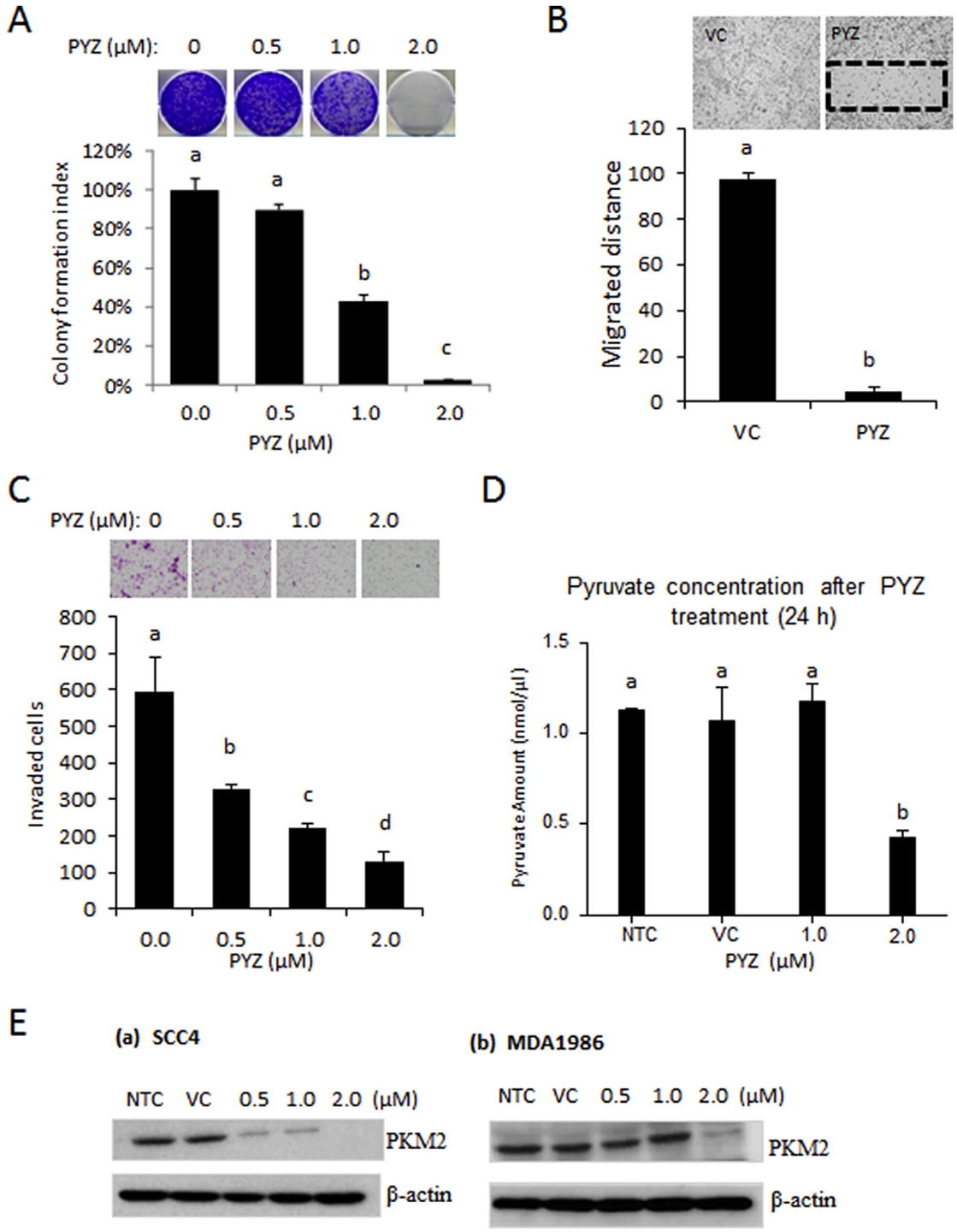

Figure 3 – (A) Colony Formation Assay. Oral cancer cells (SCC4) were treated with PYZ (0.5 μM–2 μM) for 6 days. Number of colonies formed was counted in PYZ groups or vehicle treated controls. Histogram analysis showed a significant reduction in colony forming ability of PYZ treated cells. (B) Cell Migration Assay. Histogram analysis showed significantly low number of cells in wound of PYZ treated cells ($p < 0.05$). (C) Invasion Assay. Invasion assay was performed as described in Materials and methods. Bar graphs showed a decrease in invasion potential of PYZ treated cells as compared to vehicle treated controls. (D) Estimation of pyruvate in PYZ treated cells. Pyruvate concentration was measured in SCC4 cells after the treatment of PYZ, compared with no treatment group, vehicle control, 1 μM and 2 μM shows a decrease with the 2 μM treated group. (E) Western blot analysis. Western blot analysis showed a decrease in PKM2 level in (a) SCC4 and (b) MDA1986 in a dose dependent manner. β-Actin served as a loading control. The bar graph data were presented as mean ± SEM. Treatment groups denoted by different letters represent a significant difference at $p < 0.05$ (ANOVA followed by Fisher's LSD test).

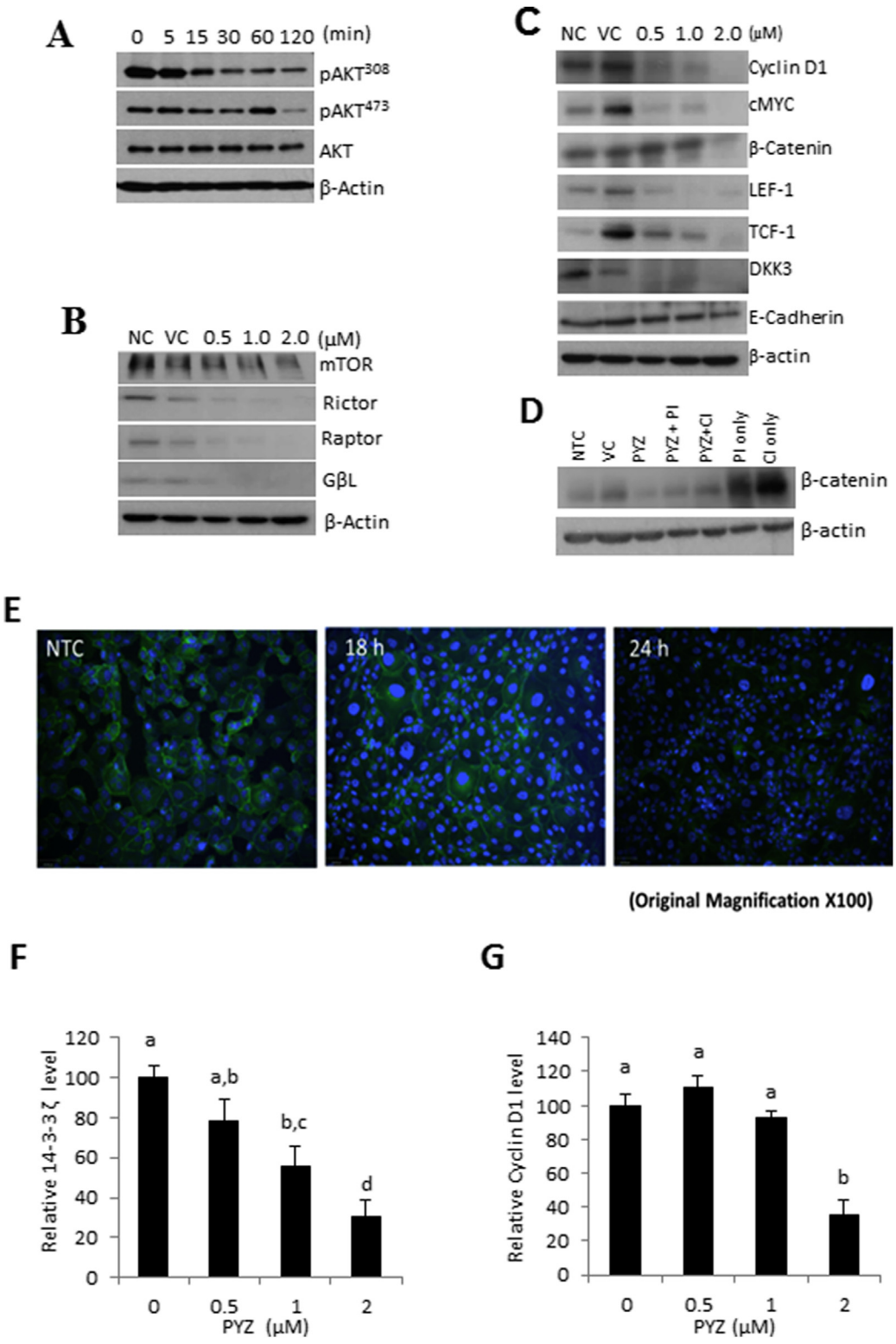

Figure 4 – (A) Western blot analysis. Western blot analysis showed a decrease in levels of pAkt^{308} and pAkt^{473}, while total Akt levels remain unchanged on treatment of PYZ (2 μM) in a time dependent manner. (B) Western blot analysis. Western blot analysis showed an alteration in mTOR, Rictor, Raptor, and GβL; β-actin served as a loading control. (C) Western blot analysis. Dose dependent treatment of SCC4 cells with PYZ (0.5 μM–2 μM) did not show any change in E-cadherin levels in PYZ treated cells; but showed a decrease in expression of β-catenin, LEF-1, TCF-1, DKK3, c-Myc and Cyclin D1. β-Actin served as a loading control. (D) Western blot analysis. Western blot analysis showed no degradation or significant loss of β-catenin on treatment with PYZ in presence of proteasomal (PI) or caspase inhibitor (CI) in comparison to no treatment or vehicle control but a significant change with respect to PYZ treatment only. (E) Confocal Laser Scan Microscopy. Image showed loss of membranous and cytoplasmic β-catenin from PYZ treated SCC4 cells in 18 h–24 h. DAPI indicates nuclei and green fluorescence signal by

significant reduction of pyruvate levels in comparison with the untreated control cells (Figure 3D). Pyruvate kinase M2 (PKM2) expression is often up-regulated in cancer cells (Hayes and Grandis, 2015; Lui et al., 2013). Since PYZ treatment led to cell death, we determined if this agent can modify the level of PKM2. Oral cancer cells, SCC4 were treated with PYZ in a dose dependent manner for 24 h. PYZ treatment led to a dose-dependent reduction in PKM2 levels in both SCC4 and MDM1986 cells (Figure 3E and Supplementary Figure S5). Thus, PYZ treatment results in reduced PKM2 expression in OSCC cells.

3.6. Treatment with PYZ alters PI3K/AKT/mTOR and Wnt/β-catenin signaling in OSCC cells

PI3K/Akt/mTOR (mammalian target of rapamycin) and Wnt/β-catenin signaling cascades along with their downstream effector proteins play an important role in oral cancer (Ahn et al., 2008; Hayes and Grandis, 2015; Kaur et al., 2013; Lui et al., 2013; Macha et al., 2011a,b; Matta and Ralhan, 2009; Molinolo et al., 2009, 2012; Ralhan et al., 2009b; Rohatgi et al., 2005; Sawhney et al., 2007; Sharma et al., 2006). To determine whether PYZ treatment modifies these signaling pathways, SCC4 were treated with PYZ (2 μM), and cell lysates were subjected to Western blot analysis. PYZ exposure led to a time dependent decrease in Akt phosphorylation at Thr308 ($pAkt^{308}$) and Ser473 ($pAkt^{473}$). In contrast, the total levels of Akt protein were not altered (Figure 4A and Supplementary Figure S6A). Treatment with PYZ also affected the expression of mTOR signaling related protein in oral cancer cells. PYZ-treated oral cancer cells showed decreased mTOR expression and its downstream targets, including Raptor, Rictor, and GβL (Figure 4B and Supplementary Figure S6B). Thus, PYZ alters AKT/mTOR signaling in OSCC cells.

Next, we examined whether PYZ affects signaling of Wnt/β-catenin pathway, a down-stream target of Akt activation. We found that PYZ treatment led to loss of expression of the major proteins involved in Wnt/β-catenin signaling including β-catenin, its nuclear interaction partners TCF1 and LEF1, its upstream regulator Dickkopf family (DKK3), and their down-stream targets cyclin D1 and c-Myc on treatment with PYZ (0–2 μM, 48 h) in SCC4 cells (Figure 4C, Supplementary Figure S6C). Decrease in β-catenin expression was also shown in MDA1986 (Supplementary Figure S3). Further, Confocal laser scan microscopy also demonstrated the loss of both membrane and cytoplasmic β-catenin protein expression with PYZ treatment for 18 h in SCC4 cells (Figure 4E), confirming that PYZ treated SCC4 cells lead to a decrease in β-catenin level (Figure 4C). Despite the altered Wnt/β-catenin signaling in PYZ-treated cells, no significant difference in expression of E-cadherin was observed these cells (Figure 4C, Supplementary Figure S6C).

To elucidate mechanism by which PYZ causes loss of β-catenin, the effect of PYZ on β-catenin expression was also investigated in the presence of proteasomal (5 μg/μl) or caspase inhibitor (10 μg/ml) in SCC4 cells. The reduction in β-catenin expression was most pronounced on PYZ treatment for 48 h (Figure 4D and Supplementary Figure S6D), though decreased levels of β-catenin were observed in the presence of PYZ and proteasomal inhibitor or caspase inhibitor as compared to treatment with the proteasomal inhibitor or caspase inhibitor alone. These findings suggest PYZ dependent degradation of β-catenin is likely to be the result of partial activation of proteasome or caspases. Together, we showed that PYZ treatment in OSCC altered activation of Wnt/β-catenin pathway in oral cancer.

3.7. PYZ alters mRNA expression of 14-3-3ζ and cyclin D1 in oral cancer cells

PYZ was shown to decrease the protein level of 14-3-3ζ (Figure 2F), which we have shown earlier to be involved in Bcl-2 dependent apoptosis in oral cancer cells (Macha et al., 2010), and cyclin D1 (Figure 4C), one of the downstream targets of Wnt/β-catenin signaling. We further examined whether PYZ regulated their expression at the transcriptional level in OSCC. Realtime PCR analysis showed mRNA levels of 14-3-3ζ and cyclin D1 were decreased in SCC4 cells by PYZ treatment for 24 h in a dose dependent manner (Figure 4F and G). PYZ inhibited the expression of 14-3-3ζ and cyclin D1 at both protein level and mRNA level, indicating these two genes are PYZ targets in OSCC to induce cell apoptosis and anti-proliferation effect through inhibiting AKT/mTOR and Wnt/β-catenin signaling pathways.

3.8. Treatment with PYZ delays tumor growth in xenograft model

To determine the anti-tumor activity of PYZ *in vivo*, we injected SCC4 cells in mice subcutaneously, and tumors were allowed to develop to a size ~200 mm^3, before they were treated with vehicle control (0.05% DMSO) or PYZ (1 mg/kg b.wt.). We found that tumor growth was significantly delayed in PYZ treated mice (mean tumor volume, 316.24 ± 58.5 mm^3) in comparison with vehicle control group (mean tumor volume 479.6 ± 16.9 mm^3, one sample t-test, $p < 0.001$, Figure 5A). PYZ treatment markedly reduced the growth of SCC4 derived tumor xenografts in mice during the course of treatment and had a significant tumoristatic effect (Figure 5B, i and ii). Importantly, no significant weight loss was observed in PYZ-treatment group, as compared to the vehicle control groups (Supplementary Figure S7). On gross examination of liver and microscopic examination of H&E stained liver slides no obvious signs of oncocytic necrosis or fibrosis were observed in PYZ-treated mice (Figure 5C, i and ii). No gross or microscopic kidney lesions were observed in PYZ treated mice (Figure 5C, iii and iv). To further investigate the toxicity of PYZ treatment, if any, sera samples from

FITC represents β-catenin. The original magnification is 100×. (F) 14-3-3ζ and (G) Cyclin D1 expression was decreased in a dose (0–2 μM) dependent manner in SCC4 cells with PYZ treatment for 24 h as assessed via qPCR. For qPCR measurement, GAPDH was used for data normalization. Data are shown as the mean ± SEM. Treatment groups denoted by different letters represent a significant difference at $p < 0.05$ (ANOVA followed by Fisher's LSD test).

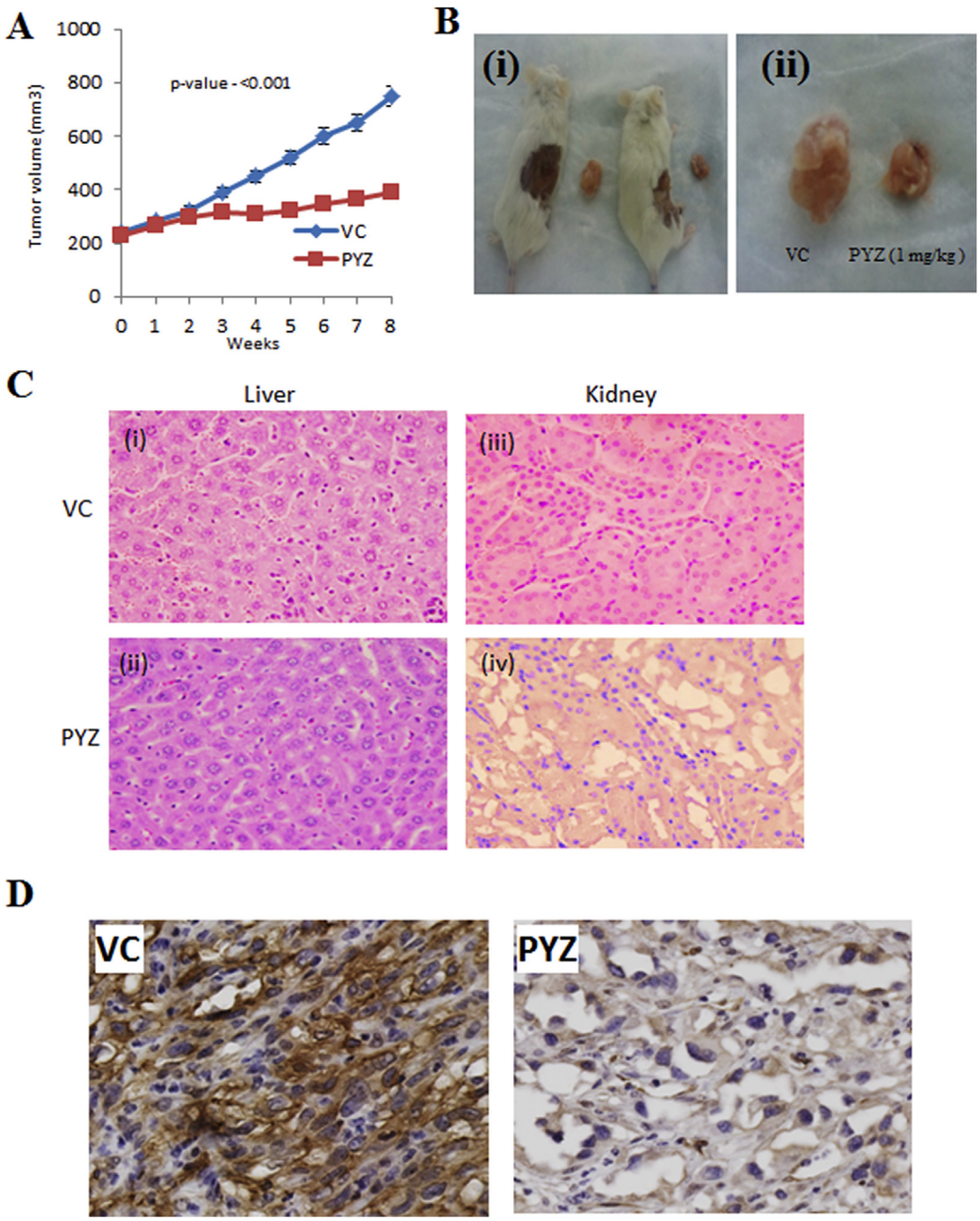

Figure 5 – (A) PYZ delays growth of SCC4 tumor xenografts. Tumor xenografts developed in the flanks of NOD/SCID/CRL mice after administration with PYZ (1 mg/kg) intraperitoneally weekly for 6 weeks. One sample t-test shows a decrease in tumor volume in the mice with PYZ treatment compared to vehicle controls. (B) PYZ inhibits growth of SCC4 tumor xenografts (i) & (ii): Significant reduction in tumor size in mice treated with PYZ was observed as compared to vehicle controls. (C) Hematoxylin and eosin stained liver and kidney tissue sections. Histology of liver and kidney tissues obtained at the conclusion of the *in vivo* study. Sections were stained with hematoxylin–eosin (H&E). (i), Section of liver after the treatment with vehicle control; (ii), Section of liver after the treatment with PYZ; (iii), Section of the kidney after the treatment with vehicle control; and (iv), Section of kidney after the treatment with PYZ. No oncocytic necrosis or fibrosis was observed in both kidney and liver after the treatment with PYZ. The original magnification is 40×. (D) Immunohistochemical analysis of β-catenin expression in PYZ treated tumor xenografts in immunocompromised mice. The expression of cytoplasmic β-catenin in PYZ treated tumor xenografts in mice was reduced in comparison with tumors in the vehicle control mice. Quantitative image analysis using the Visiopharm software revealed 67% cytoplasm positive tumor cells in xenografts from the vehicle treated mice; in comparison 8% cytoplasm positive tumor cells were observed in xenografts from the PYZ treated mice confirming significant reduction in β-catenin expression in PYZ treated mice xenografts. The original magnification is 40×.

treated and untreated mice were analyzed to compare clinical chemistry profiles, hematology and organ function tests by Charles River Laboratories, Quebec, Canada. Notably, no significant differences were observed on any of these parameters among PYZ treated and vehicle control mice (Supplementary Tables T1 and T2). Thus, treatment of PYZ at 1 mg/kg b.wt., *in vivo* allows tumor reduction without conferring significant toxicity to host animals.

One of the effects of PYZ treatment *in vitro* is the down-regulation of β-catenin (Figure 4C, D & F). Consistent with these data, we also observed reduced expression of β-catenin in PYZ treated tumor xenografts in immunocompromised mice in comparison with tumors in the vehicle control mice (Figure 5D). Quantitative image analysis using the Visiopharm software revealed 67% cytoplasm positive tumor cells in xenografts from the vehicle treated mice; in comparison 8% cytoplasm positive tumor cells were observed in xenografts from PYZ treated mice confirming significant reduction in β-catenin expression in PYZ treated mice xenografts, suggesting β-catenin is a molecular target of PYZ *in vivo* as well. Together these data suggest PYZ has anti-tumor activity against OSCCs *in vivo*.

4. Discussion

The objective of this study was to identify novel compounds that will serve as an effective alternative to current chemotherapeutic agents for OSCC patients. Using HTS assays, we captured <1% of the potent candidate anti-proliferative small molecule inhibitors for oral cancer cells. Further studies on these small molecule inhibitors combined with their efficacy led to identification of PYZ as the most potent anti-proliferative agent for OSCC using oral cancer cells *in vitro* and mouse xenograft *in vivo*. Based on our findings, PYZ has anticancer effects on both HPV+ and HPV− as well as wild type *p53* and mutant *p53* harboring oral cancer cells. Treatment with PYZ resulted in cleavage of caspase 3, caspase 9 and PARP (DNA repair enzyme), suggesting activation of intrinsic mitochondrial pathway of apoptosis in PYZ-treated OSCC cells. In support of this, our results demonstrated increased expression of the pro-apoptotic proteins (Bax, Bid and Bad) and decreased levels of anti-apoptotic proteins (Bcl-xl, Bcl-2 and PUMA) as well as 14-3-3σ and 14-3-3ζ on PYZ treatment. 14-3-3 family of proteins play an important role in abrogating apoptosis by sequestering phospho-Bad (pBad, Ser136) in cytoplasm, thereby inhibiting intrinsic pathway of apoptosis (Macha et al., 2010). Simultaneous loss of both the 14-3-3 isoforms (ζ and σ), and increased expression of pro-apoptotic proteins (Bad and Bax) on treatment with PYZ results in inhibition of proliferation and induction of apoptosis.

In breast cancer and ovarian cancer cells, Zn-mediated apoptosis involved oxidative stress and mitochondrial translocation of Bax (Alam and Kelleher, 2012). Similarly, Zn induced oxidative stress and translocation of apoptosis-inducing factor (AIF) into the nucleus resulting in caspase-independent apoptosis in pancreatic adenocarcinoma (Donadelli et al., 2009). PYZ-induced ERK activation generated reactive oxygen species (ROS), contributing to DNA damage and mitochondrial stress (Carraway and Dobner, 2012). However, in acute myeloid leukemia (AML) cells, PYZ induced apoptosis independent of DNA damage, ROS and protein misfolding (Tailler et al., 2012). PYZ treatment resulted in loss of NFκB expression and its target genes in AML cells (Tailler et al., 2012). Treatment of prostate cancer cells with PYZ resulted in a rapid decline in cellular ATP levels associated with membrane blebbing (Carraway and Dobner, 2012). Interestingly, increasing intracellular zinc concentrations in laryngeal cells increased apoptotic cell death at lower doses (150 μM) but resulted in necrotic cell death at higher dose (300–750 μM) (Rudolf et al., 2003). Although the detailed mechanism of PYZ induced apoptosis in cancer cells remains to be elucidated, zinc ionophores including PYZ have been suggested to target cancer cells by increasing intracellular Zn^{2+} concentration.

We also investigated the effect of PYZ treatment on major signaling cascades (PI3K/Akt/mTOR and Wnt/β-catenin) regulating cellular proliferation, growth, survival, metabolism in OSCCs. We have earlier shown Akt promotes cell survival and proliferation by phosphorylation of Bad on S136, resulting in its sequestration in cytoplasm by 14-3-3ζ in oral cancer cells (Macha et al., 2010). This prevents release of cytochrome c from mitochondria, activation of caspase 9 and hence apoptosis. Notably, our current results revealed lower levels of pAkt (Thr^{308} and Ser^{473}) in PYZ treated cells within 2 h of PYZ treatment, supporting PYZ induced apoptosis. In addition, activated Akt signaling also controls cell growth and proliferation in response to extracellular mitogenic signals via mTOR signaling (Molinolo et al., 2012). We observed decreased expression of mTOR protein complex including mTOR, Rictor, Raptor, and GβL in PYZ treated cells. These findings suggest that PI3K/AKT and mTOR signaling pathways play important role in PYZ anti-cancer efficacy in oral cancer cells.

The deregulation of Wnt/β-catenin signaling is another important event in development and progression of oral cancer (Gonzalez-Moles et al., 2014; Molinolo et al., 2009). Of note, changes in β-catenin protein levels and its sub-cellular localization are crucial in the regulation of β-catenin/TCF transcriptional activity (Valenta et al., 2012). Stability and nuclear accumulation of β-catenin is mainly influenced by glycogen synthase kinase 3β (GSK3β) (Valenta et al., 2012). Activated Wnt signaling leads to the phosphorylation of the disheveled (Dsh) protein which, through its association with axin, prevents glycogen synthase kinase 3β (GSK3β) from phosphorylating critical substrates including β-catenin. This causes stability and accumulation of nuclear β-catenin leading to transcriptional activation of target genes, cyclin D1 and c-Myc (Valenta et al., 2012). Our data revealed lower levels of β-catenin and its associated nuclear proteins TCF-1 and LEF-1 resulting in reduced transcriptional activity in PYZ treated oral cancer cells. This was supported by the decreased expression of its target proteins, cyclin D1 and c-Myc. Further, our results revealed PYZ decreased β-catenin expression was inhibited in the presence of proteasomal or pan-caspase inhibitor. Loss of membranous β-catenin was observed before complete loss of expression as revealed by immunofluorescence. Importantly, our *in vivo* studies also showed that PYZ treated OSCC tumor xenografts from SCC4 cells in immunocompromised mice showed reduced β-catenin in tumor cells as compared to tumor xenografts from vehicle control group of mice, confirming our *in vitro* findings.

We also observed lower levels of pyruvate and loss of PKM2, an important glycolytic enzyme in PYZ-treated OSCC cells revealing effects of PYZ on metabolism and glycolysis in particular in cancer cells. Earlier reports have shown a marked decrease in cellular ATP levels, suggesting the inhibitory effects of Zn^{2+} on glycolysis and oxidative

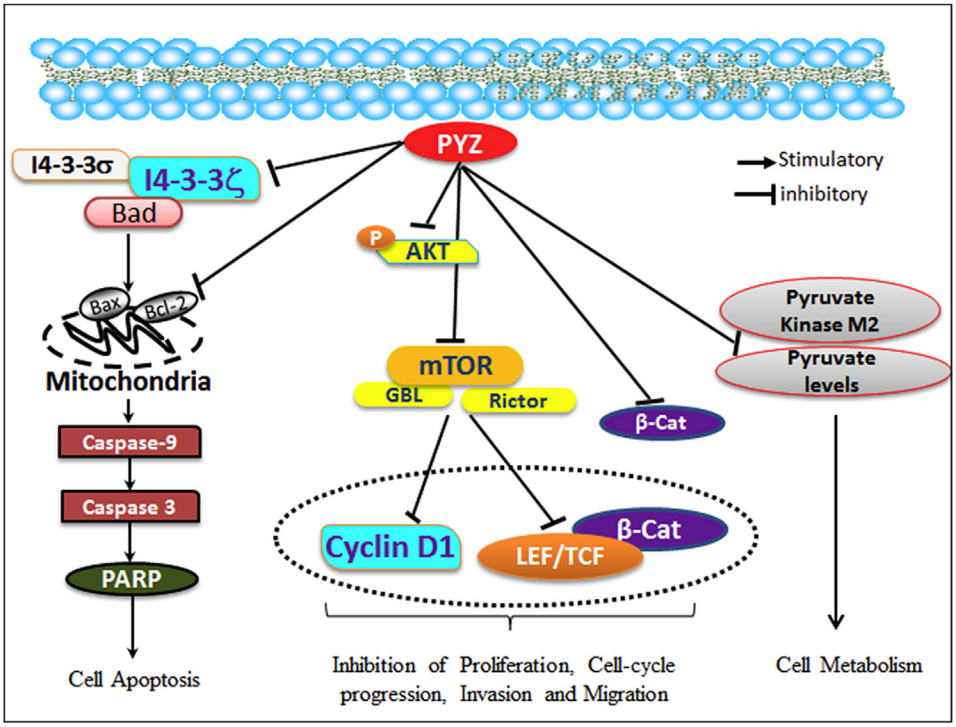

Figure 6 – Working model of pyrithione zinc in oral cancer. PYZ modulates directly or indirectly the major proteins implicated in oral carcinogenesis, proliferation, invasion, migration, cell cycle progression, apoptosis and metabolism. PYZ induced upregulation of pro-apoptotic BAX and BAD is indicative of release of cytochrome C from mitochondria which further activates Caspase-3, Caspase-9 and PARP, suggesting caspase dependent apoptosis. Treatment with PYZ also downregulated the expression of 14-3-3ζ and 14-3-3σ proteins, which have been previously shown to be implicated in oral carcinogenesis. PYZ treatment also decreased pAkt levels and downregulated DKK3, β-catenin, LEF1, TCF1, and its target cyclin D1 and c-Myc suggesting inhibition of Wnt/β-catenin signaling pathway. PYZ treatment also downregulated mTOR, GβL, Rictor, and Raptor, suggesting inhibition of the mTOR pathway in PYZ treated oral cancer cells. PYZ inhibited pyruvate levels and PKM2, suggesting inhibition of the metabolic activity in PYZ treated oral cancer cells.

phosphorylation (Dineley et al., 2003). Zn^{2+} has been reported to inhibit several metabolic enzymes including glyceraldehyde-3-phosphate dehydrogenase (GAPDH), pyruvate dehydrogenase, α-ketoglutarate dehydrogenase and m-aconitase (Dineley et al., 2003). Together, decline in ATP levels, oxidative damage, DNA fragmentation and activation of pro-apoptotic cascade results in PYZ induced apoptosis in OSCC cells. In support of our *in vitro* data demonstrating efficiency of PYZ as a novel drug for OSCC, *in vivo* mouse xenograft studies revealed markedly reduced growth of the tumor without any noticeable change in weight of PYZ–treated animal groups. Moreover, clinical chemistry profiles, hematology and organ function tests of PYZ treated mice did not show any toxicity in PYZ treated mice. These pre-clinical findings suggest that PYZ has a therapeutic effect on oral cancer *in vivo*. The cellular pathways and proteins targeted by PYZ are schematically depicted in a hypothetical model as shown in Figure 6.

In support of cellular signaling cascades and novel proteins suggested as targets of PYZ in OSCCs, our data in human OSCCs and dysplasia clinical samples have demonstrated their relevance in development and progression of oral carcinogenesis (Kaur et al., 2014, 2013; Matta et al., 2008; Ralhan et al., 2009a; Tripathi et al., 2010; Winter et al., 2011). We showed OSCC patients showing overexpression of 14-3-3σ, 14-3-3ζ and/or decreased expression of membranous β-catenin revealed reduced disease free survival. Further, loss of β-catenin membrane staining associated with enhanced tumor invasiveness, late clinical stage, nodal metastasis, and poor prognosis (Kaur et al., 2013). These findings were supported by similar reports from other groups subsequently (Liao et al., 2011; Roesch-Ely et al., 2007; Winter et al., 2011). In support of our study, abnormal β-catenin expression was reported in progression of oral carcinomas, lymph node metastasis and cell proliferation in OSCCs and was suggested to be valuable for diagnosis of metastasis in OSCCs, late clinical stage, early local recurrence and poor prognosis in OSCC (de Aguiar et al., 2007).

In conclusion, a high-throughput screen seeking novel anticancer agents for oral cancer led to re-purposing of the anti-fungal agent, PYZ as a potential anti-proliferative agent for OSCC. The *in vitro* studies demonstrated PYZ treatment of oral cancer cells activated pro-apoptotic signaling cascades targeting multiple cellular proteins providing in depth understanding of its mechanism of action in oral cancer. *In vivo* mouse xenograft oral cancer models used to investigate the anticancer effect of PYZ underscored its pre-clinical anticancer efficacy suggesting potential use in treatment of OSCC with a high potency and low toxicity.

Authors' contributions

RR conceptualized the study, contributed to the study design and to the manuscript. GS, AM, GF and RS conducted the experimental work. GS, AM and GF carried out the statistical analysis and had access to the raw data. PGW, AD and RR provided the infrastructure. The manuscript was drafted by GS, AM, GF and RS, edited by GF and RR and submitted for comments to all the authors of this study. The investigators incorporated their suggestions and all authors approved the final version of the manuscript.

Disclosure of potential conflicts of interest

The authors declared no potential conflicts of interest.

Acknowledgments

The financial support of this work from Canadian Cancer Society Research Institute (Innovation grant # 701781), Canadian Institutes of Health Research for Chair in Advanced Cancer Diagnostics (RR), and Alex and Simona Shnaider Chair in Thyroid Cancer (PGW) are gratefully acknowledged. We thank Drs. Vejaynthi Pethe and Jatinder Kaur for their assistance in enabling us to make the study feasible in the initial stages of this research work.

Appendix A. Supplementary data

Supplementary data related to this article can be found online at http://dx.doi.org/10.1016/j.molonc.2015.05.005.

REFERENCES

Ahn, K.S., Sethi, G., Sung, B., Goel, A., Ralhan, R., Aggarwal, B.B., 2008. Guggulsterone, a farnesoid X receptor antagonist, inhibits constitutive and inducible STAT3 activation through induction of a protein tyrosine phosphatase SHP-1. Cancer Res. 68, 4406–4415.

Alam, S., Kelleher, S.L., 2012. Cellular mechanisms of zinc dysregulation: a perspective on zinc homeostasis as an etiological factor in the development and progression of breast cancer. Nutrients 4, 875–903.

Audrey, R.C.B., 2012. Head and Neck: squamous cell carcinoma: an overview. Atlas Genet. Cytogenet. Oncol. Haematol. 16, 145–155.

Brana, I., Siu, L.L., 2012. Locally advanced head and neck squamous cell cancer: treatment choice based on risk factors and optimizing drug prescription. Ann. Oncol. 23 (Suppl. 10) x178–85.

Carraway, R.E., Dobner, P.R., 2012. Zinc pyrithione induces ERK- and PKC-dependent necrosis distinct from TPEN-induced apoptosis in prostate cancer cells. Biochim. Biophys. Acta 1823, 544–557.

Costello, L.C., Franklin, R.B., 2011. Zinc is decreased in prostate cancer: an established relationship of prostate cancer! J. Biol. Inorg. Chem. 16, 3–8.

de Aguiar Jr., A., Kowalski, L.P., de Almeida, O.P., 2007. Clinicopathological and immunohistochemical evaluation of oral squamous cell carcinoma in patients with early local recurrence. Oral Oncol. 43, 593–601.

Dineley, K.E., Votyakova, T.V., Reynolds, I.J., 2003. Zinc inhibition of cellular energy production: implications for mitochondria and neurodegeneration. J. Neurochem. 85, 563–570.

Donadelli, M., Dalla Pozza, E., Scupoli, M.T., Costanzo, C., Scarpa, A., Palmieri, M., 2009. Intracellular zinc increase inhibits p53(−/−) pancreatic adenocarcinoma cell growth by ROS/AIF-mediated apoptosis. Biochim. Biophys. Acta 1793, 273–280.

Ertekin, M.V., Koc, M., Karslioglu, I., Sezen, O., Taysi, S., Bakan, N., 2004. The effects of oral zinc sulphate during radiotherapy on anti-oxidant enzyme activities in patients with head and neck cancer: a prospective, randomised, placebo-controlled study. Int. J. Clin. Pract. 58, 662–668.

Ferlay, J., Soerjomataram, I., Ervik, M., Dikshit, R., Eser, S., Mathers, C., Rebelo, M., Parkin, D.M., Forman, D., Bray, F., 2012. Cancer Incidence and Mortality Worldwide: IARC CancerBase No. 11 [Internet]. GLOBOCAN 2012 v1.0 Lyon, France: International Agency for Research on Cancer; 2013. Available from: http://globocan.iarc.fr.

Fong, L.Y., Jiang, Y., Farber, J.L., 2006. Zinc deficiency potentiates induction and progression of lingual and esophageal tumors in p53-deficient mice. Carcinogenesis 27, 1489–1496.

Fu, G., Peng, C., 2011. Nodal enhances the activity of FoxO3a and its synergistic interaction with Smads to regulate cyclin G2 transcription in ovarian cancer cells. Oncogene 30, 3953–3966.

Fu, G., Ye, G., Nadeem, L., Ji, L., Manchanda, T., Wang, Y., Zhao, Y., Qiao, J., Wang, Y.L., Lye, S., Yang, B.B., Peng, C., 2013. MicroRNA-376c impairs transforming growth factor-beta and nodal signaling to promote trophoblast cell proliferation and invasion. Hypertension 61, 864–872.

Gomez, D.R., Zhung, J.E., Gomez, J., Chan, K., Wu, A.J., Wolden, S.L., Pfister, D.G., Shaha, A., Shah, J.P., Kraus, D.H., Wong, R.J., Lee, N.Y., 2009. Intensity-modulated radiotherapy in postoperative treatment of oral cavity cancers. Int. J. Radiat. Oncol. Biol. Phys. 73, 1096–1103.

Gonzalez-Moles, M.A., Ruiz-Avila, I., Gil-Montoya, J.A., Plaza-Campillo, J., Scully, C., 2014. Beta-catenin in oral cancer: an update on current knowledge. Oral Oncol. 50, 818–824.

Grinshtein, N., Datti, A., Fujitani, M., Uehling, D., Prakesch, M., Isaac, M., Irwin, M.S., Wrana, J.L., Al-Awar, R., Kaplan, D.R., 2011. Small molecule kinase inhibitor screen identifies polo-like kinase 1 as a target for neuroblastoma tumor-initiating cells. Cancer Res. 71, 1385–1395.

Harari, P.M., Wheeler, D.L., Grandis, J.R., 2009. Molecular target approaches in head and neck cancer: epidermal growth factor receptor and beyond. Semin. Radiat. Oncol. 19, 63–68.

Hayes, D.N., Grandis, J.R., 2015. Comprehensive genomic characterization of head and neck squamous cell carcinomas. Nature 517, 576–582.

Kaur, J., Matta, A., Kak, I., Srivastava, G., Assi, J., Leong, I., Witterick, I., Colgan, T.J., Macmillan, C., Siu, K.W., Walfish, P.G., Ralhan, R., 2014. S100A7 overexpression is a predictive marker for high risk of malignant transformation in oral dysplasia. Int. J. Cancer 134, 1379–1388.

Kaur, J., Sawhney, M., DattaGupta, S., Shukla, N.K., Srivastava, A., Walfish, P.G., Ralhan, R., 2013. Clinical significance of altered expression of beta-catenin and E-cadherin in oral dysplasia and cancer: potential link with ALCAM expression. PLoS One 8, e67361.

Kim, M.S., Li, S.L., Bertolami, C.N., Cherrick, H.M., Park, N.H., 1993. State of p53, Rb and DCC tumor suppressor genes in human oral cancer cell lines. Anticancer Res. 13, 1405–1413.
Kumar, A., Chatopadhyay, T., Raziuddin, M., Ralhan, R., 2007. Discovery of deregulation of zinc homeostasis and its associated genes in esophageal squamous cell carcinoma using cDNA microarray. Int. J. Cancer 120, 230–242.
Lamore, S.D., Wondrak, G.T., 2011. Zinc pyrithione impairs zinc homeostasis and upregulates stress response gene expression in reconstructed human epidermis. Biometals 24, 875–890.
Lansford, C.D., Grenman, R., Bier, H., Somers, K.D., Kim, S.Y., Whiteside, T.L., Clayman, G.L., Welkoborsky, H.I., Carey, T.E., 1999. Head and Neck Cancers. Kluwer Academic Publishers, Norwell, MA, pp. 185–255.
Liao, K.A., Tsay, Y.G., Huang, L.C., Huang, H.Y., Li, C.F., Wu, T.F., 2011. Search for the tumor-associated proteins of oral squamous cell carcinoma collected in Taiwan using proteomics strategy. J. Proteome Res. 10, 2347–2358.
Lin, L.C., Que, J., Lin, K.L., Leung, H.W., Lu, C.L., Chang, C.H., 2008. Effects of zinc supplementation on clinical outcomes in patients receiving radiotherapy for head and neck cancers: a double-blinded randomized study. Int. J. Radiat. Oncol. Biol. Phys. 70, 368–373.
Lin, Y.S., Lin, L.C., Lin, S.W., 2009. Effects of zinc supplementation on the survival of patients who received concomitant chemotherapy and radiotherapy for advanced nasopharyngeal carcinoma: follow-up of a double-blind randomized study with subgroup analysis. Laryngoscope 119, 1348–1352.
Lui, V.W., Hedberg, M.L., Li, H., Vangara, B.S., Pendleton, K., Zeng, Y., Lu, Y., Zhang, Q., Du, Y., Gilbert, B.R., Freilino, M., Sauerwein, S., Peyser, N.D., Xiao, D., Diergaarde, B., Wang, L., Chiosea, S., Seethala, R., Johnson, J.T., Kim, S., Duvvuri, U., Ferris, R.L., Romkes, M., Nukui, T., Kwok-Shing Ng, P., Garraway, L.A., Hammerman, P.S., Mills, G.B., Grandis, J.R., 2013. Frequent mutation of the PI3K pathway in head and neck cancer defines predictive biomarkers. Cancer Discov. 3, 761–769.
Macha, M.A., Matta, A., Chauhan, S., Siu, K.M., Ralhan, R., 2010. 14-3-3 zeta is a molecular target in guggulsterone induced apoptosis in head and neck cancer cells. BMC Cancer 10, 655.
Macha, M.A., Matta, A., Chauhan, S.S., Siu, K.W., Ralhan, R., 2011a. Guggulsterone (GS) inhibits smokeless tobacco and nicotine-induced NF-kappaB and STAT3 pathways in head and neck cancer cells. Carcinogenesis 32, 368–380.
Macha, M.A., Matta, A., Chauhan, S.S., Siu, K.W., Ralhan, R., 2011b. Guggulsterone targets smokeless tobacco induced PI3K/Akt pathway in head and neck cancer cells. PLoS One 6, e14728.
Malo, N., Hanley, J.A., Cerquozzi, S., Pelletier, J., Nadon, R., 2006. Statistical practice in high-throughput screening data analysis. Nat. Biotechnol. 24, 167–175.
Martens-de Kemp, S.R., Dalm, S.U., Wijnolts, F.M., Brink, A., Honeywell, R.J., Peters, G.J., Braakhuis, B.J., Brakenhoff, R.H., 2013. DNA-bound platinum is the major determinant of cisplatin sensitivity in head and neck squamous carcinoma cells. PLoS One 8, e61555.
Masters, J.R.W., Palsson, B., 1999. Human Cell Culture. Hand book II Cancer cell lines, pp. 244–257.
Matta, A., DeSouza, L.V., Ralhan, R., Siu, K.W., 2010. Small interfering RNA targeting 14-3-3zeta increases efficacy of chemotherapeutic agents in head and neck cancer cells. Mol. Cancer Ther. 9, 2676–2688.
Matta, A., DeSouza, L.V., Shukla, N.K., Gupta, S.D., Ralhan, R., Siu, K.W., 2008. Prognostic significance of head-and-neck cancer biomarkers previously discovered and identified using iTRAQ-labeling and multidimensional liquid chromatography-tandem mass spectrometry. J. Proteome Res. 7, 2078–2087.
Matta, A., Ralhan, R., 2009. Overview of current and future biologically based targeted therapies in head and neck squamous cell carcinoma. Head Neck Oncol. 1, 6.
Molinolo, A.A., Amornphimoltham, P., Squarize, C.H., Castilho, R.M., Patel, V., Gutkind, J.S., 2009. Dysregulated molecular networks in head and neck carcinogenesis. Oral Oncol. 45, 324–334.
Molinolo, A.A., Marsh, C., El Dinali, M., Gangane, N., Jennison, K., Hewitt, S., Patel, V., Seiwert, T.Y., Gutkind, J.S., 2012. mTOR as a molecular target in HPV-associated oral and cervical squamous carcinomas. Clin. Cancer Res. 18, 2558–2568.
Myers, J.N., Holsinger, F.C., Jasser, S.A., Bekele, B.N., Fidler, I.J., 2002. An orthotopic nude mouse model of oral tongue squamous cell carcinoma. Clin. Cancer Res. 8, 293–298.
Ralhan, R., Desouza, L.V., Matta, A., Chandra Tripathi, S., Ghanny, S., Dattagupta, S., Thakar, A., Chauhan, S.S., Siu, K.W., 2009a. iTRAQ-multidimensional liquid chromatography and tandem mass spectrometry-based identification of potential biomarkers of oral epithelial dysplasia and novel networks between inflammation and premalignancy. J. Proteome Res. 8, 300–309.
Ralhan, R., Pandey, M.K., Aggarwal, B.B., 2009b. Nuclear factor-kappa B links carcinogenic and chemopreventive agents. Front. Biosci. (Schol. Ed.) 1, 45–60.
Roesch-Ely, M., Nees, M., Karsai, S., Ruess, A., Bogumil, R., Warnken, U., Schnolzer, M., Dietz, A., Plinkert, P.K., Hofele, C., Bosch, F.X., 2007. Proteomic analysis reveals successive aberrations in protein expression from healthy mucosa to invasive head and neck cancer. Oncogene 26, 54–64.
Rohatgi, N., Kaur, J., Srivastava, A., Ralhan, R., 2005. Smokeless tobacco (khaini) extracts modulate gene expression in epithelial cell culture from an oral hyperplasia. Oral Oncol. 41, 806–820.
Rudolf, E., Rudolf, K., Radocha, J., Peychl, J., Cervinka, M., 2003. The role of intracellular zinc in modulation of life and death of Hep-2 cells. Biometals 16, 295–309.
Sakai, E., Tsuchida, N., 1992. Most human squamous cell carcinomas in the oral cavity contain mutated p53 tumor-suppressor genes. Oncogene 7, 927–933.
Sawhney, M., Rohatgi, N., Kaur, J., Shishodia, S., Sethi, G., Gupta, S.D., Deo, S.V., Shukla, N.K., Aggarwal, B.B., Ralhan, R., 2007. Expression of NF-kappaB parallels COX-2 expression in oral precancer and cancer: association with smokeless tobacco. Int. J. Cancer 120, 2545–2556.
Scully, C., Bagan, J.V., 2008. Recent advances in Oral Oncology 2007: imaging, treatment and treatment outcomes. Oral Oncol. 44, 211–215.
Sharma, C., Kaur, J., Shishodia, S., Aggarwal, B.B., Ralhan, R., 2006. Curcumin down regulates smokeless tobacco-induced NF-kappaB activation and COX-2 expression in human oral premalignant and cancer cells. Toxicology 228, 1–15.
Smith, K.M., Datti, A., Fujitani, M., Grinshtein, N., Zhang, L., Morozova, O., Blakely, K.M., Rotenberg, S.A., Hansford, L.M., Miller, F.D., Yeger, H., Irwin, M.S., Moffat, J., Marra, M.A., Baruchel, S., Wrana, J.L., Kaplan, D.R., 2010. Selective targeting of neuroblastoma tumour-initiating cells by compounds identified in stem cell-based small molecule screens. EMBO Mol. Med. 2, 371–384.
Soussi, T., 2007. Handbook of p53 Mutation in Cell Lines. Version 1.0 07/2007.
Taccioli, C., Chen, H., Jiang, Y., Liu, X.P., Huang, K., Smalley, K.J., Farber, J.L., Croce, C.M., Fong, L.Y., 2012. Dietary zinc deficiency fuels esophageal cancer development by inducing a distinct inflammatory signature. Oncogene 31, 4550–4558.
Tailler, M., Senovilla, L., Lainey, E., Thepot, S., Metivier, D., Sebert, M., Baud, V., Billot, K., Fenaux, P., Galluzzi, L.,

Boehrer, S., Kroemer, G., Kepp, O., 2012. Antineoplastic activity of ouabain and pyrithione zinc in acute myeloid leukemia. Oncogene 31, 3536–3546.

Tripathi, S.C., Matta, A., Kaur, J., Grigull, J., Chauhan, S.S., Thakar, A., Shukla, N.K., Duggal, R., DattaGupta, S., Ralhan, R., Siu, K.W., 2010. Nuclear S100A7 is associated with poor prognosis in head and neck cancer. PLoS One 5, e11939.

Tzivion, G., Gupta, V.S., Kaplun, L., Balan, V., 2006. 14-3-3 proteins as potential oncogenes. Semin. Cancer Biol. 16, 203–213.

Valenta, T., Hausmann, G., Basler, K., 2012. The many faces and functions of beta-catenin. Embo J. 31, 2714–2736.

Winter, J., Pantelis, A., Reich, R., Jepsen, S., Allam, J.P., Novak, N., Wenghoefer, M., 2011. Risk estimation for a malignant transformation of oral lesions by S100A7 and Doc-1 gene expression. Cancer Investig. 29, 478–484.

Zhang, J.H., Chung, T.D., Oldenburg, K.R., 1999. A simple statistical parameter for use in evaluation and validation of high throughput screening assays. J. Biomol. Screen. 4, 67–73.